A new software toolkit for optical apportionment of carbonaceous aerosol

Tommaso Isolabella[1,2], Vera Bernardoni[3], Alessandro Bigi[4], Marco Brunoldi[1,2], Federico Mazzei[1,2], Franco Parodi[2], Paolo Prati[1,2], Virginia Vernocchi[2], Dario Massabò[1,2]

[1] Physics Department, University of Genoa, 16146 Genoa, Italy
[2] I.N.F.N., Division of Genoa, 16146 Genoa, Italy
[3] Dipartimento di Fisica, Università degli Studi di Milano, and I.N.F.N. Division of Milan, 20133 Milan, Italy
[4] Department of Engineering 'Enzo Ferrari', University of Modena and Reggio Emilia, 41125 Modena, Italy

Correspondence to: Dario Massabò (dario.massabo@ge.infn.it)

Abstract. Instruments measuring aerosol light absorption, such as the Aethalometer and the Multi-Wavelength Absorbance Analyzer (MWAA), have been extensively used to characterize optical absorption of atmospheric particulate matter. Data retrieved with such instruments can be analysed with mathematical models to apportion different aerosol sources (Aethalometer model) and components (MWAA model). In this work we present an upgrade to the MWAA optical apportionment model. In addition to the apportionment of the absorption coefficient b_{abs} in its components (Black Carbon and Brown Carbon) and sources (Fossil Fuel and Wood Burning), the extended model allows the retrieval of the Absorption Ångström Exponent of each component and source, thereby avoiding initial assumptions regarding these parameters. We also present a new open-source software toolkit, the MWAA Model Toolkit, written in both Python and R, that performs the entire apportionment procedure.

1 Introduction

Atmospheric Particulate Matter (PM) plays an important role in environmental issues such as human health, air quality and climate change (Seinfeld and Pandis, 2016). Several chemical species and aggregates, present in the atmosphere, affect the energy balance of the Earth system by absorbing and scattering solar radiation (Laj et al., 2020). A variety of sources contribute to the emission of light absorbing or scattering PM: their identification and quantification are necessary to mitigate the harmful effects of PM, especially in the climate change issue.

Between other constituents, Black Carbon (BC) and Brown Carbon (BrC) are the most light-absorbing components of PM (Bond et al., 2013). BC consists of fractal-like chains of submicron particles, and it is formed by incomplete combustion processes. Due to the wavelength independence of the imaginary part of its refractive index, it is a strong light absorber across the entire visible range. BrC represents a more elusive class of organic carbonaceous compounds whose defining characteristic is to absorb radiation more efficiently at shorter visible bands than at longer wavelengths, where its absorption is considered negligible (Poeschl, 2003; Andreae and Gelencser, 2006). The composition of BrC is still poorly understood, due to its chemical complexity and spatiotemporal variability; it consists of a number of molecular weight compounds, generally prone to oxidation and chemically unstable (Forrister et al., 2015). BrC is emitted directly through combustion of biomass but can also be formed as a product of secondary processes in the atmosphere (Liu et al., 2015, Tang et al., 2016).

Other aerosol compounds exhibit strong, albeit more selective, light-interaction properties. One such example is mineral dust, which is the most widespread aerosol type in terms of total mass, with a consequent important impact on the Earth's

energy balance due to its light absorption properties (Alfaro et al., 2009, Caponi et al., 2015 Schepanski, 2018, Di Biagio et al, 2019). However, in this work, we restrict our attention to carbonaceous aerosol and its sources.

In general, the spectral dependence of light absorption by small particles can be parameterized with a power-law function. In particular, the aerosol absorption coefficient b_{abs} can be written as a function of the wavelength of the incoming radiation as $b_{abs}(\lambda) = c\lambda^{-\alpha}$, where c is a proportionality factor and α, the Absorption Ångström Exponent (AAE), defines the spectral dependence of the absorption. Different aerosol types correspond to different values of α, which has been shown to depend on particle size, morphology, chemical composition, and mixing/ageing state (Moosmüller et al 2011; Utry et al 2014). For BC in its ideal form (spherical particles with no wavelength-dependence of the imaginary part of the refractive index), the literature is consistent in indicating the α value of 1, both for real-world (Bond and Bergstrom, 2006) and produced in controlled conditions (Vernocchi et al., 2022) samples, whereas much more variation is encountered in the value of α for BrC, with reported values ranging up to 9.5 (Hoffer et al., 2006; Harrison et al., 2013; Lack and Langridge; 2013). This is likely due to the broader range of chemical composition and effects of ageing. Intermediate values of α are observed for aerosols containing both BC and BrC (Massabò et al., 2019). This significant difference in the wavelength-dependent behaviour of light-absorbing components can be used as an efficient tool for the source and component apportionment of light-absorbing aerosol.

Source apportionment models exploiting the power-law behaviour of b_{abs} have been successfully applied to multi-λ measurements of absorption. The Aethalometer model (Sandradewi et al., 2008), allows the apportionment of the absorption coefficient to two different sources, namely Fossil Fuel (FF) and Wood Burning (WB), exploiting the different α that characterizes the aerosol produced by the two sources. The MWAA (Multi-Wavelength Absorbance Analyzer) model extends the Aethalometer model by explicitly including the apportionment of optical absorption due to BC and BrC, resulting in an algorithm that allows the differentiation of both aerosol sources and components, based on at least $5-\lambda$ absorption measurements (Massabò et al., 2015; Bernardoni et al., 2017). Both the Aethalometer model and the MWAA model are effective in apportioning aerosol absorption, but they have a conceptual drawback: the values of some physical parameters must be fixed prior to the analysis in order to run the algorithm. These parameters are the α for FF and WB (α_{FF} and α_{WB} for the Aethalometer model, and, in addition, α_{BC} for the MWAA model). Since the α depends on a variety of factors, as mentioned above, fixing these exponents for the analysis, according to the literature, can lead to errors, since the actual value of these exponents may be different for the specific aerosol analysed. The only way to avoid this problem is to retrieve these crucial parameters by using information obtained by independent techniques/methods (e.g., Levoglucosan, ^{14}C, receptor models, others), as stated in several recent publications in the literature (Massabò et al., 2015; Martinsson et al., 2017; Titos et al., 2017, Helin et al., 2018; Ivančič et al., 2022).

In this work we propose: 1) a toolkit that implements a revised version of the original MWAA model, as published in Massabò et al., 2015. This toolkit has been rewritten and optimized in Python and R, and is available for use by the scientific community. It has been also extended with the possibility to use an arbitrary number of spectrally resolved absorption coefficients, as long as at least 5 wavelengths are available. This model is self-consistent and can be applied to purely optical data without the need of any other information. 2) A~~a~~n upgrade to the original MWAA model that directly allows source and component apportionments of absorption data without the need to set any parameters before running the model. This is achieved by performing the apportionment analysis along with a correlation study with ~~other,~~ independent measurements ~~of aerosol properties,~~ such as chemical speciation or elemental composition. The parameters are then automatically set by the algorithm, based on the values that give the best correlation with the independent measurements. ~~We also present a~~ The new software toolkit presented here is written in two of the most widely used scientific programming languages, Python and R, to perform this analysis automatically. Output of the presented toolkit

(MWAA_MT) are the following quantities: α_{FF}, α_{WB}, α_{BC}, α_{BrC}, and the carbonaceous masses for fossil fuels and wood burning: EC_{FF}/OC_{FF}, and EC_{WB}/OC_{WB}, respectively, where EC (OC) stands for Elemental (Organic) Carbon. Finally, to demonstrate the capability of the upgraded model, we provide an example application to data published elsewhere (Bernardoni et al., 2017).

2 Model description

The MWAA model has been extensively described elsewhere (Massabò et al., 2015). Here we will only report the main points to establish the notation and describe the upgrades.

The measured aerosol absorption coefficient b_{abs} at different wavelengths is decomposed in two different ways:

$$b_{abs}(\lambda) = b_{abs}^{BC}(\lambda) + b_{abs}^{BrC}(\lambda) = A\lambda^{-\alpha_{BC}} + B\lambda^{-\alpha_{BrC}} \quad (1)$$

and

$$b_{abs}(\lambda) = b_{abs}^{FF}(\lambda) + b_{abs}^{WB}(\lambda) = A'\lambda^{-\alpha_{FF}} + B'\lambda^{-\alpha_{WB}} \quad (2)$$

Equation (1) represents the decomposition of the measured aerosol absorption coefficient, at each wavelength, into its contributions due to carbonaceous components, BC and BrC. Both species are assumed to absorb radiation according to a negative power law $b_{abs}(\lambda) \propto \lambda^{-\alpha}$, with a different absorption exponent for BC (α_{BC}) and BrC (α_{BrC}).

Equation (2) has the same structure as the Aethalometer apportionment model (Sandradewi 2008), whereby the absorption coefficient is decomposed into contributions from different sources, FF and WB. As in Eq. (1), these terms are also assumed to contribute to the total optical absorption following negative power law whose exponents are different for FF (α_{FF}) and WB (α_{WB}).

The parameters A, B, A' and B' are scaling factors proportional to the Mass Absorption Cross-section (MAC) of each component. In the original MWAA model, all but one of the exponents (α_{BrC}) are fixed to appropriate values according to the literature (Sandradewi et al., 2008; Favez et al., 2010; Herich et al., 2011: Harrison et al., 2013; Massabò et al., 2015; Zotter et al., 2017; Forello et al., 2019), most commonly $\alpha_{BC} = \alpha_{FF} = 1$ and $\alpha_{WB} = 1.8$ or 2. Then, the multi-λ measurements of b_{abs} are fitted using Eq. (1) and (2), obtaining A, B, A', B' and α_{BrC}. The contribution of the different sources and species to the optical absorption is obtained as follows:

$$\begin{aligned} b_{abs}^{BC,WB}(\lambda) &= (A - A')\lambda^{-\alpha_{BC}} \\ b_{abs}^{BC,FF}(\lambda) &= A'\lambda^{-\alpha_{BC}} \\ b_{abs}^{BrC}(\lambda) &= B\lambda^{-\alpha_{BrC}} \end{aligned} \quad (3)$$

The upgraded model we present eliminates the need to arbitrarily specify α_{BC}, α_{FF} and α_{WB} by instead adjusting their values so that the apportioned contributions found in (3) have the best correlation with independent measurements. Figure 1 shows a streamlined version of the upgraded MWAA model, in which the independent measurement for the adjustment of the exponents is the levoglucosan content in the sample, as determined by chromatography. Levoglucosan is a strong tracer for biomass burning (Simoneit et al., 1999) and should therefore correlate well with b_{abs}^{BrC} and $b_{abs}^{BC,WB}$.

The three parameters α_{BC}, α_{FF} and α_{WB} are each varied within their range, while the others are held constant. In the first step, α_{BC} is varied in the set $\{0.8, 0.9, 1.0, 1.1, 1.2\}$. For each α_{BC} value, Eq. (1) is used to fit the data and b_{abs}^{BrC} is calculated

for the shortest available wavelength, using Eq. (3). The coefficient of determination R^2 for a linear regression between b_{abs}^{BrC} and the levoglucosan concentration for all samples is calculated, and the α_{BC} value that maximizes R^2 is selected. In the second step, α_{WB} is set to 2 and a similar procedure as described for the first step is performed for on α_{FF}. Finally, in the third step, the procedure is repeated to find a best value for α_{WB}. It is worth noting that the permutation of the steps to minimize α_{FF} and α_{WB} leads to the same preprocessing results. These three steps are repeated $N = 3$ times, restricting the range of variability for the parameters in each iteration to increase the accuracy of the search for the best values. To avoid statistically insignificant results, and to obtain a more robust result, a tolerance parameter Δ is introduced. If the increase of R^2 in each minimization routine is less than the tolerance, the previous value of the relevant α is retained.

In addition to the component and source apportionment of the optical absorption coefficient, the MWAA model provides a method to perform the apportionment of EC and OC masses to the fossil fuel and wood burning contributions:

$$
\begin{aligned}
EC_{FF} &= \frac{b_{abs}^{BC,FF}(\lambda_l)}{b_{abs}(\lambda_l) - b_{abs}^{BrC}(\lambda_l)}\, EC \\
EC_{WB} &= \frac{b_{abs}^{BC,WB}(\lambda_l)}{b_{abs}(\lambda_l) - b_{abs}^{BrC}(\lambda_l)}\, EC \\
EC &= EC_{FF} + EC_{WB} \qquad (4) \\
OC_{FF} &= k_1 b_{abs}^{BC,FF}(\lambda_l) + OC_{NC} \\
OC_{WB} &= k_2 b_{abs}^{BrC}(\lambda_s) + OC_{NC} \\
OC &= OC_{FF} + OC_{WB} + OC_{NC}
\end{aligned}
$$

In the above equations, λ_l and λ_s represent the longest and shortest wavelengths for which a measurement is available, respectively; OC_{NC} is the organic carbon produced by biogenic sources which is considered optically inactive; k_1 and k_2 are coefficients, in $g\ m^{-2}$, obtained by a linear regression of Eq. (4.3) and (4.4), in subsets of samples in which the OC concentration is low (for k_1) and high (for k_2). The coefficients k_1 and k_2 are related to the Mass Absorption Cross-

sections (MACs) of BC and BrC, respectively, and to the ratios OC_{FF}/BC_{FF} and OC_{WB}/BrC. For more details on the mass apportionment procedure, see Massabò et al., 2015.

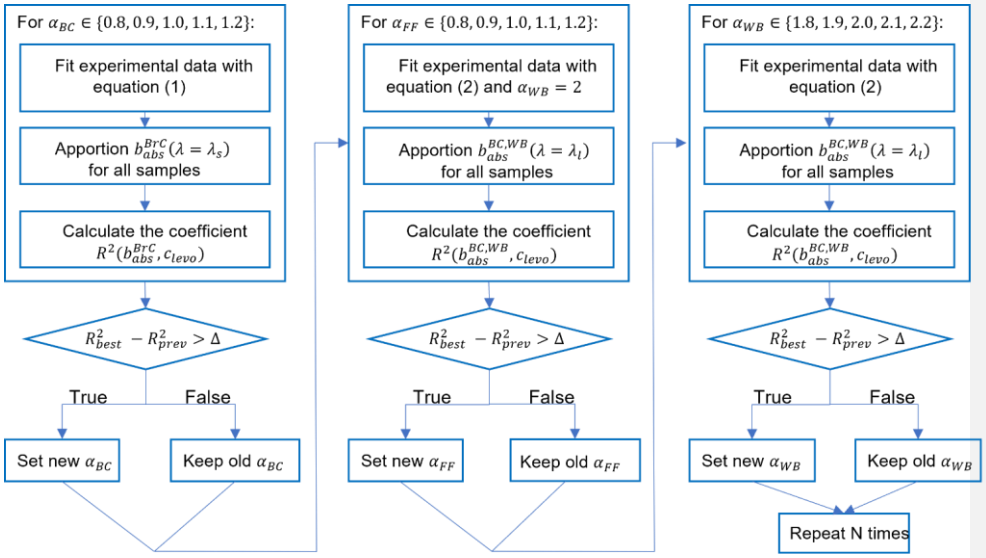

Figure 1: Flowchart illustrating the pre-processing step in the improved MWAA model. c_{levo} is the levoglucosan concentration in the samples, R^2 is the coefficient of determination in the linear regression, and the subscripts best and prev refer to, respectively, the best correlation in the present iteration, and the best correlation in the previous iteration relative to the same α; Δ is a tuneable tolerance that prevents statistically insignificant fluctuations to assume a physical meaning.

3 Software features

The software toolkit that performs the above-mentioned analysis has been released in the public domain. It can be installed via a standalone executable file (**download link**) or directly from source (**github link**). Currently, it can only be run in a Linux distribution (for example Ubuntu or Linux Mint).

MWAA_MT (the MWAA Model Toolkit) can perform optical and mass apportionment of data obtained with instruments measuring light absorption at least at five wavelengths, such as a multi − λ Aethalometer.

The toolkit works in four separate steps:

- Step I — It retrieves the best values for the three parameters α_{BC}, α_{FF} and α_{WB} following the method detailed in the Sect. 2.
- Step II — The values of A, B, A', B' and α_{BrC} are obtained from fitting Eq. (1) and (2) with the remaining exponents fixed to the best values found in the previous step.
- Step III — Equations (3) are employed to apportion the absorption coefficient at every wavelength.
- Step IV — Following Eq. (4) the mass apportionment is performed for each sample.

The first step of the analysis is the most innovative aspect of the tool we introduce here, since the three values of α_{BC}, α_{FF} and α_{WB} are directly retrieved by the toolkit itself. However, if data from at least one independent analysis (e.g., Levoglucosan, ^{14}C, PMF, etc.) are not available, the user can still set these three parameters manually. In addition, the mass apportionment step is optional depending on the availability of carbonaceous mass measurements: if EC and OC are not available for the samples, the user can decide to skip the fourth step.

Similarly, the user can set many of the analysis hyperparameters. To perform the first step of the analysis, the current version of the toolkit allows comparison of the optical apportionment with levoglucosan measurements, as described above. Future versions of MWAA_MT will likely allow the user to choose between different types of preprocessing analysis, considering different types of data such as ^{14}C measurements or source apportionment results obtained with independent techniques such as Positive Matrix Factorization or Multilinear Engine ME-2 receptor models. Another possibility could be to constrain the model to maximise the correlation with tracers of traffic emission such as NO_x.

Any number of samples can be provided for an analysis run; for the main optical apportionment procedure, steps II and III, each sample is processed independently, whereas for the steps I and IV the entire dataset is considered for the regression analyses. Therefore, extra care must be taken to avoid entering obvious outliers as input to the software, and the analysis may need to be run twice, with the first run serving to weed out potential outliers and adjust the range of parameter variation.

4 Example of application: black and brown carbon optical apportionment of MWAA data

As an example of the application of MWAA_MT, we examine the results of the apportionment of two datasets previously published (Bernardoni et al., 2017). The first dataset is from a sampling campaign conducted in fall/winter 2014 in Propata, a rural site in northern Italy, while the second dataset is from a campaign conducted in winter 2016 at an urban background site in Milan, one of the largest cities in Italy. In these campaigns, PM10 samples were collected on quartz fibre filters, with each filter sampled (for 48h in Propata, for 12h in Milan) and then analysed with the MWAA instrument to obtain the wavelength resolved absorption coefficients of the aerosol. All samples were analysed by liquid chromatography (HPLC-PAD) to determine the Levoglucosan concentration (Piazzalunga et al., 2010). No information on chemical speciation (except Levoglucosan) was available at the two sites; the average PM10 concentration measured at Propata and Milan was 8.3 ± 6.0 μg m^{-3} and 68.3 ± 25.6 μg m^{-3}, respectively. Further details on the measurements can be found in Bernardoni et al. (2017). In the current study, we apply the updated MWAA model (MWAA_MT) to 28 samples from the Propata campaign (hereinafter referred to as "P" samples) and 25 samples from the Milan campaign ("AIN" samples). The aim of the comparison is to verify whether the particulate sampled in a rural area has a different optical behaviour than the aerosol sampled in an urban area. The following steps were performed identically for both datasets.

ha formattato: Tipo di carattere: Non Corsivo

ha formattato: Tipo di carattere: Non Corsivo

ha formattato: Tipo di carattere: Symbol

ha formattato: Tipo di carattere: Non Corsivo

ha formattato: Apice

ha formattato: Tipo di carattere: Non Corsivo

ha formattato: Tipo di carattere: Non Corsivo

4.1 Preliminary: comparison with levoglucosan concentrations

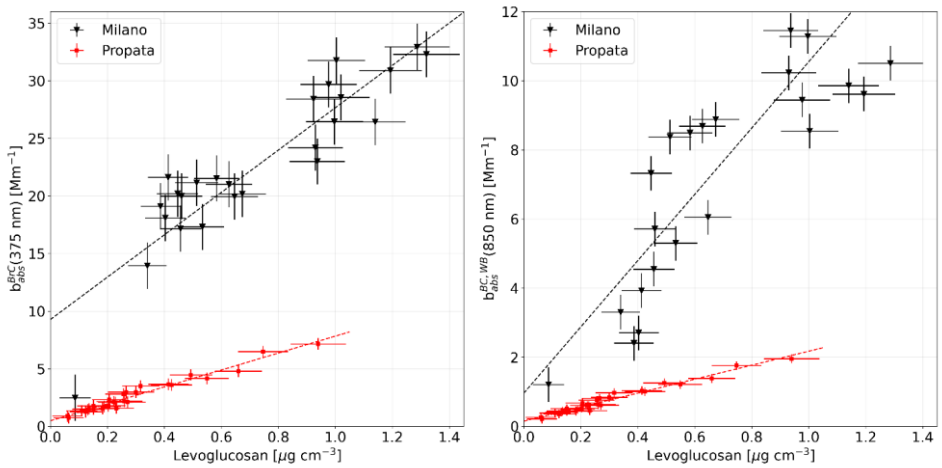

Figure 2: Correlation between the levoglucosan concentration and the apportioned absorption coefficient of BrC at 375 nm (left plot), and the absorption coefficient of BC due to wood burning at 850 nm (right plot). The rural site, Propata (red dots) exhibits a higher correlation than the urban site Milan (black triangles).

To determine the goodness of the apportionment procedure even without the extra pre-processing step, default values for the free parameters were chosen ($\alpha_{BC} = \alpha_{FF} = 1,\ \alpha_{WB} = 2$) and the standard MWAA model for optical apportionment (steps II and III above) was run. Figure 2 shows the correlation plots between the levoglucosan concentration and the relevant apportionment results, namely $b_{abs}^{BrC}(\lambda = 375\ nm)$ and $b_{abs}^{BC,WB}(\lambda = 850\ nm)$. The linear regression equations and coefficients of determination are given in Table 1.

Table 1: Results of the correlation analysis between the apportioned data and the independent measurement, in this case levoglucosan concentration. The goodness-of-fit of the correlation, represented by the coefficient of determination R^2, is much higher in Propata than in Milan.

Location	Absorption	Fit equation y = mx + q {m} = $Mm^{-1}\mu g^{-1}cm^3$ {q} = Mm^{-1}	R^2
Milan	$b_{abs}^{BrC}(\lambda = 375\ nm)$	$m = 18.4 \pm 1.8,$ $q = 9.3 \pm 1.4$	0.82
Milan	$b_{abs}^{BC,WB}(\lambda = 850\ nm)$	$m = 9.6 \pm 1.1,$ $q = 1.0 \pm 0.9$	0.75
Propata	$b_{abs}^{BrC}(\lambda = 375\ nm)$	$m = 7.3 \pm 0.3,$ $q = 0.48 \pm 0.10$	0.96
Propata	$b_{abs}^{BC,WB}(\lambda = 850\ nm)$	$m = 2.02 \pm 0.07,$ $q = 0.15 \pm 0.03$	0.97

4.2 Analysis step I

As described in Sect. 2, the first step of the upgraded apportionment model is to find the values of the absorption exponents that maximise the correlation between some of the model's output values and one or more independent techniques. In this case, since the concentration of levoglucosan (hereinafter c_l) was measured on all samples, the following set of optimizations ('Levoglucosan' analysis preset in MWAA_MT) was carried out:

- vary α_{BC} to maximise the correlation between $b_{abs}^{BrC}(\lambda = 375\ nm)$ and c_l;
- vary α_{FF} to maximise the correlation between $b_{abs}^{BC,WB}(\lambda = 850\ nm)$ and c_l;
- vary α_{WB} to maximise the correlation between $b_{abs}^{BC,FF}(\lambda = 850\ nm)$ and c_l.

The resulting sets of exponents were $(\alpha_{BC}, \alpha_{FF}, \alpha_{WB})^P = (1.00 \pm 0.05;\ 1.00 \pm 0.02;\ 2.00 \pm 0.05)$ for Propata and $(\alpha_{BC}, \alpha_{FF}, \alpha_{WB})^M = (0.90 \pm 0.05;\ 0.90 \pm 0.02;\ 1.70 \pm 0.05)$ for Milan. Figure 3 shows the variation of the R^2 coefficient, in the two sites: the change of α_{WB} value does not produce any sizeable impact in the analysis of the rural dataset whereas in Milan the best choice turned out to be $\alpha_{WB} = (1.70 \pm 0.05)$. Through the sensitivity tests we performed on the preprocessing step, we discovered that the apportioned optical absorption coefficients can vary by up to 10% by adjusting the values of the α parameters within their uncertainty brackets. We estimated the uncertainty of the α parameters by considering the steepness of the R^2 vs. α curves. The curve of α_{FF} is very steep, which led us to estimate an uncertainty of 0.02, whereas the R^2 vs α curves for the other two parameters were flatter, indicating a larger uncertainty for these parameters.

ha formattato: Tipo di carattere: Non Corsivo

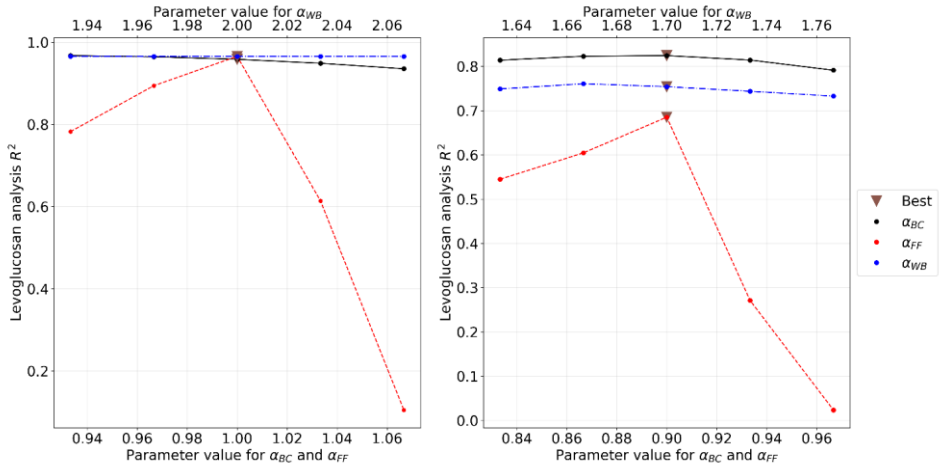

Figure 3: Trend of the R^2 correlation coefficient between the levoglucosan concentration and the apportioned optical absorption coefficient vs. the value of the α exponents: Propata (left panel) and Milan dataset (right panel). The values of α parameter which maximize the R^2 coefficient, are marked with a brown triangle. The plots are shown only for the last iteration of the preprocessing step.

This justifies the choice of setting $\alpha_{WB} = 2.0$ for the rural site, while the same choice is less robust for the urban site, where $\alpha_{WB} = 1.7$ would be the more appropriate setting. The analysis confirms the usual choice of $\alpha_{BC} = 1.0$ for the rural site, while $\alpha_{BC} = 0.9$ gives the optimal value for the urban dataset, possibly indicating a further reprocessing and ageing of pure BC particles in the urban environment (Minderytė et al, 2022). As with α_{FF}, the analysis yields $\alpha_{FF} = 1.0$ and $\alpha_{FF} = 0.9$ for the rural and urban site/dataset, respectively.

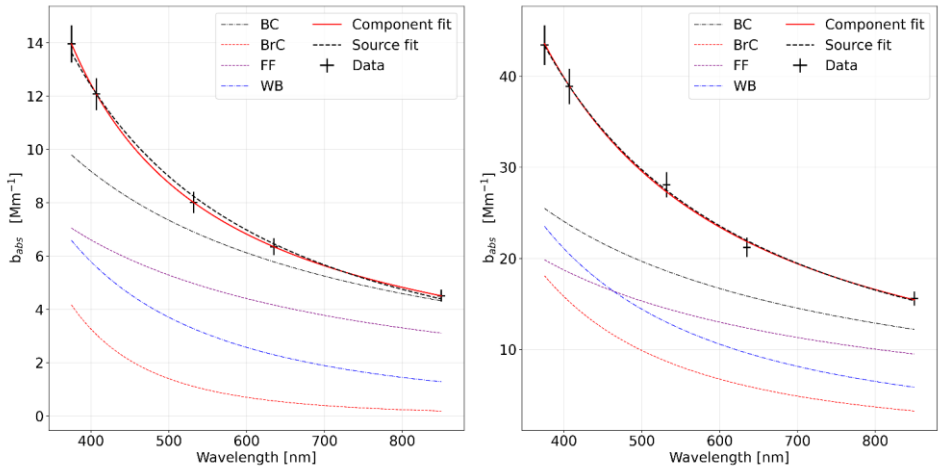

Figure 4: Absorption coefficient plots for a representative sample from the rural site in Propata (left) and the urban site in Milan (right). The experimental data points are marked with uncertainty crosses. Superimposed on the graphs are the results of the fits carried out with the two different decompositions from Sect. 1.

4.3 Analysis step II

The parameters found in Step I are then fixed for each dataset, and a complete double fit of the experimental data is performed for each sample following Eq. (1) and (2). An example of such fits for a sample belonging to each of the two datasets is shown in Fig. 4.

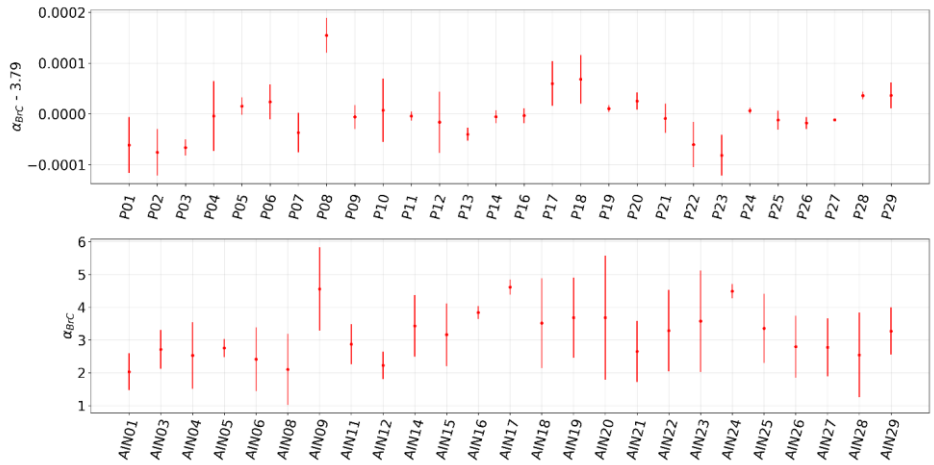

Figure 5: Values of the parameter α_{BrC} for all the samples in the datasets: Propata/rural (top) and Milan/urban (bottom).

One of the parameters determined during the fitting procedure is α_{BrC}. Its range of variability over the entire dataset and the uncertainty associated with its value allow an estimation of the physical and chemical variability of the analysed particulate. Figure 5 shows the determined values of α_{BrC} for the entire sampling period at the two sites. At a rural site such as Propata, where wood burning is the predominant source of carbonaceous particulate in the atmosphere during winter, BrC corresponds to a well-defined sub-category of organic carbon and its absorption properties are therefore constant. This is confirmed by the very small range of variation in the value of α_{BrC} obtained for all Propata samples, with $\alpha_{BrC}^{P} = 3.79 \pm 0.04$, where the uncertainty is due to inherent systematic variations in the minimization routine. At the Milan urban site, the range of variability of α_{BrC} is much higher. This can be due to the fact that the urban aerosol is much more complex and contains a larger number of organic carbon compounds from different types of wood burned under different conditions, some of which could affect the optical behaviour of the aerosol. Moreover, stagnation conditions that favour ageing processes are typical of Milan (and the Po Valley in general): they generally lead to an increase in the molecular weight of organic matter, possibly enhancing light-absorption properties. Therefore, our model, based on this simple decomposition, does not retrieve a sharp value for α_{BrC}, since the optical properties of BrC vary strongly in Milan, unlike in Propata where the sampled particulate was comparatively simpler. The determined absorption exponent for BrC in Milan is therefore $\alpha_{BrC}^{M} = 3.5 \pm 1.1$.

4.4 Analysis step III

The optical apportionment of the absorption coefficient is performed for all available wavelengths according to Eq. (3). Figures 6 and 7 show the apportioned b_{abs} at UV (375 nm) and IR (850 nm) wavelengths for Propata and Milan, respectively. The main difference between the two sites is the correlation between b_{abs}^{BrC} and $b_{abs}^{BC,WB}$. In Propata (Fig. 6) the correlation is high, as can be inferred by the blue and black lines having the same time trend. This means that most of the BrC is produced via WB. On the other hand, in Milan (Fig. 7) this correlation is lower, and BrC cannot be entirely attributed to WB. In fact, in Milan the particulate is impacted by a number of different sources and it is heavily processed

due to stagnation. A general feature common to both datasets is the negligible absorption attributed to BrC at long wavelengths; this is consistent with previous work (Massabò et al., 2015).

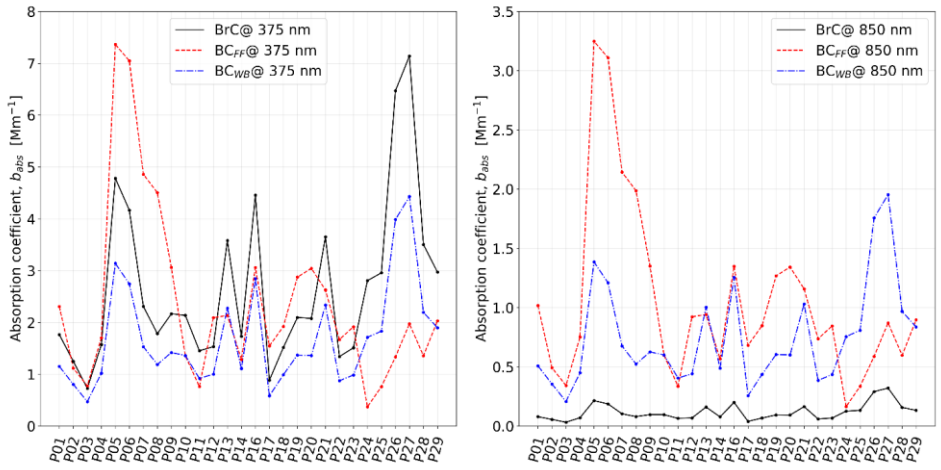

Figure 6: Temporal variability of the apportioned absorption coefficients in Propata. Each sample covers a 48h period, starting from 07/11/2014 for P01.

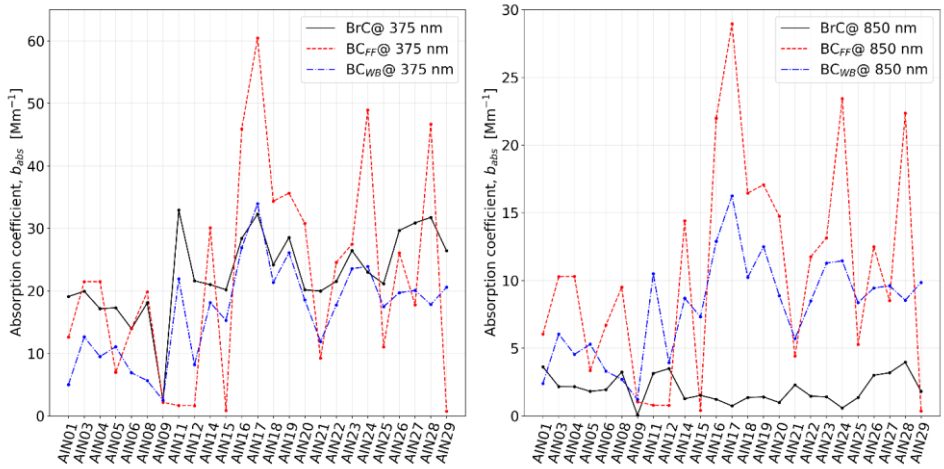

Figure 7: Temporal variability of the apportioned absorption coefficients in Milan. Each sample covers a 12h period, starting from 21:00, 21/11/2016 for AIN01.

4.5 Analysis step IV

Mass apportionment was performed for both datasets using the approach detailed in Sect. 2. The toolkit allows the user to choose to automatically determine the coefficients k_1 and k_2 from the linear regressions (see Eq. 4), or to set them manually. The latter approach is indicated when the dataset does not contain suitable candidate samples for the k_1 regression analysis (i.e. when there are no samples whose EC content is predominant as evidenced by an α close to 1), and especially when the values for k_1 and k_2 can be estimated by complementary methods or by previous analyses of aerosol samples taken at the same location during a comparable period of the year.

For this example application, the second approach was followed. For Milan, the regression coefficients were set to $k_1^M = 0.33\ g\ m^{-2}$, $k_2^M = 0.34\ g\ m^{-2}$, while for Propata they were set to $k_1^P = 0.24\ g\ m^{-2}$, $k_2^P = 0.35\ g\ m^{-2}$ as described in Bernardoni et al., 2017.

The average EC_{FF}/EC ratio turned out to be $(49\% \pm 20\%)$ and $(58\% \pm 15\%)$, and complementary EC_{WB}/EC resulted $(51\% \pm 20\%)$ and $(42\% \pm 15\%)$, respectively in Milan and Propata. For the organic aerosol, the average OC_{FF}/OC was found to be $(25\% \pm 14\%)$ and $(18\% \pm 9\%)$, while OC_{WB}/OC was $(58\% \pm 17\%)$ and $(61\% \pm 14\%)$, in Milan and Propata respectively. The non-combustion component of the organic aerosol, OC_{NC}, contributed $(17\% \pm 15\%)$ and $(21\% \pm 15\%)$ of the total OC measured in Milan and Propata. For all the reported results, the uncertainty is understood as the standard deviation in the distribution of the mass-apportioned values of EC and OC for all the samples. These results are in full agreement with those reported in Bernardoni et al., 2017.

5 Conclusions

In the aerosol community concerned with aerosol source apportionment, the possibility of apportioning carbonaceous sources by exploiting optical properties has occupied much space in recent years. The main reasons for this growing interest are the diffusion of optical instruments that ~~allow~~ are relatively easy-to-use, and allow high-time resolution measurements. The main weakness of this apportionment methodology, based on optical measurements, is the practically obligatory choice of the critical parameters necessary as input, in particular α_{WB} and α_{FF}, whose values vary considerably in the literature (Sandradewi et al., 2008; Favez et al., 2010; Herich et al., 2011: Harrison et al., 2013; Massabò et al., 2015; Zotter et al., 2017; Forello et al., 2019). In this work, we show that it is possible to perform optical source and component apportionment of carbonaceous aerosols without constraining any physical parameters with *a priori* knowledge. Instead, the upgraded model presented here (MWAA_MT) allows the determination of these parameters for any specific receptor site, provided that a measurement using an independent technique able to trace biomass burning emissions is available for comparison, also with different (lower) time resolution. This offers the advantage of an apportionment routine based entirely on experimental data, where computational parameters are automatically adjusted to best match the results with the data themselves. With this upgrade, it is possible to obtain α absorption exponents that are related to the specific site and season, allowing better characterization of future measurements at the same site or at sites with similarities (e.g., rural sites with similar geographical characteristics such as type of wood burnt). In addition, the α parameters obtained from the analysis of robust, low-time resolution samples can be used to inform and fine-tune the apportionment procedure on high-time resolution data.

~~This "pre-processing step" has shown that, for the example dataset we considered, the values for α_{BC}, α_{FF} and α_{WB} at a rural site are consistent with the literature, while in the case of an urban site, values of $\alpha_{BC} = 0.9$, $\alpha_{FF} = 0.9$ and $\alpha_{WB} = 1.7$ seem to be a more appropriate choice.~~

We have also showed how sensitive the model is to the choice of some of these parameters: in our example, in particular, the choice of α_{FF} has the greatest impact on the reliability of the subsequent apportionment. It should be emphasised that this could be a feature of these specific data/sites: other datasets could be more sensitive to the variation of another one of the free parameters. It is therefore recommended that, whenever possible, such an analysis be performed to determine the best value for any of these exponents.

We have applied this upgraded methodology to the apportionment of the optical absorption coefficient in two different sites in northern Italy. The~~is~~ "pre-processing step" has shown that, for the example dataset we considered, the values for α_{BC}, α_{FF} and α_{WB} at a rural site are consistent with the literature, while in the case of an urban site, values of $\alpha_{BC} = 0.9$, $\alpha_{FF} = 0.9$ and $\alpha_{WB} = 1.7$ seem to be a more appropriate choice. We would like to underline that the Milan case study is to be considered as a stress test of our algorithm: the context is very complex due to the presence of a large number of sources such as traffic, biomass combustion, industry, etc., in a city with over 1.3 million inhabitants. The city is also subject to major regional transport events, high PM concentrations (average PM10 value during the campaign of 68.3 ± 25.6 μg m^{-3}) and air stagnation conditions resulting in a high level of aerosol reprocessing. On the other hand, when it comes to the Propata dataset, the correlation with levoglucosan is much higher (R^2=0.96), indicating that within the experimental uncertainties the assumption that BrC is only produced by WB is satisfied.

Finally, w~~w~~e have described the operation of the new software toolkit, MWAA_MT, that we have used to perform this analysis and is made available to the scientific community.

ha formattato: Tipo di carattere: Non Corsivo

ha formattato: Tipo di carattere: Non Corsivo

Code availability

The executable version for the code presented in the article is available at ZENODO LINK. The source code is available at GITHUB LINK. Any updates will also be published on Zenodo and GitHub.

Data availability

Data will be made available on request.

Author contribution

TI and DM designed the extension to the original mathematical model. TI developed and tested the Python model code. AB translated the software to R. TI prepared the manuscript with contributions from all co-authors.

Competing interests

The authors declare that they have no conflict of interest.

Acknowledgements

We are indebted to the personnel of the mechanical workshop of the INFN division of Genoa for the continuous support in the development of scientific instrumentation.

Financial Support

This work was supported by the Italian Ministry of the University (MUR) with the PRIN2017 grant for the RHAPS project [grant number: 2017MSN7M8], by the National Institute for Nuclear Physics (INFN) through the ISPIRA project, and by the PNRR MUR - M4C2 – Investimento 1.3 - "Multi-Risk science for resilient commUnities undeR a changiNg climate (RETURN)" PE00000005 CUP HUB B63D22000670006.

~~Supplementary material~~

~~1 Toolkit implementation details (Python version)~~

~~The "MWAA_MT" toolkit is written entirely in Python 3.9 and makes use of standard libraries for scientific computing and data handling and visualization.~~

~~In particular, the data is read and manipulated using the Pandas library (Reback et al., 2022, v. 1.4.3), generic numeric tasks are handled with NumPy (Harris et al., 2020, v. 1.22.4). The power-law fits of analysis steps I and II are performed using the *optimize.curve_fit* function from the SciPy scientific computation library (Virtanen at al., 2020, v. 1.9.1), and linear regressions in steps I and IV are carried out with the *stats.linregress function* in SciPy.~~

~~Visualization of input data and of analysis results is done using the Matplotlib library (Hunter, 2007, v. 3.5.3).~~

~~2 Analysis configuration~~

~~The software can be customized to adapt the runtime analysis to the specific scenario. For example, users with no data for EC and OC concentrations can disable the mass apportionment stage of the analysis, while users can skip the preprocessing stage if independent (non-optical) measurements are not available. In addition, many parameters of each analysis stage can be tuned separately.~~

~~The configuration must be specified in a file written in the JSON format of *option_name:value*, usually named *config.json*. A template for such file, containing all the necessary options, can be found at **link**. The configuration file is divided into five sections, relating to the input and output file paths, the analysis steps to perform and their specific parameters.~~

~~The analysis necessitates one input data file, in .csv format, for which a template can be found at **link**. The file has to contain the data in the format of one row per sample, with the first column being the sample ID, the subsequent columns containing the data for optical absorption at the wavelength indicated by each column header, and optionally the EC and OC concentrations and other available measurements that need to be considered in the analysis.~~

2.1 Pre-processing step: presets

For the optional analysis step I, a correlation with levoglucosan concentration measurements can be booked in order to optimize the values for α_{BC}, α_{FF} and α_{WB}.

- The levoglucosan correlation analysis optimizes α_{BC} by maximising the correlation between c_i, the levoglucosan concentration, and $b_{abs}^{BrC}(\lambda = \lambda_{min})$, α_{FF} and α_{WB} by maximising the correlation between c_i and $b_{abs}^{BC,WB}(\lambda = \lambda_{max})$.

2.2 Pre-processing step: α_{BC} swipe

As an additional check for the value of α_{BC} to be used in the subsequent analysis steps, an optional α_{BC} swipe analysis can be booked. It consists of varying α_{BC} in a wide range of values centred around 1.0. For each α_{BC} value, the fit in Eq. (1) is performed for all samples, then the average α_{BrC} and its standard deviation are computed, as shown in Fig. S1 for Propata and Milan. This analysis can give additional corroboration to a particular choice of a value for α_{BC} based on the physical assumption that BrC in a particular location (especially rural areas) and time of year has a defined chemical composition and therefore its optical absorption (e.g., its α) should show little variation.

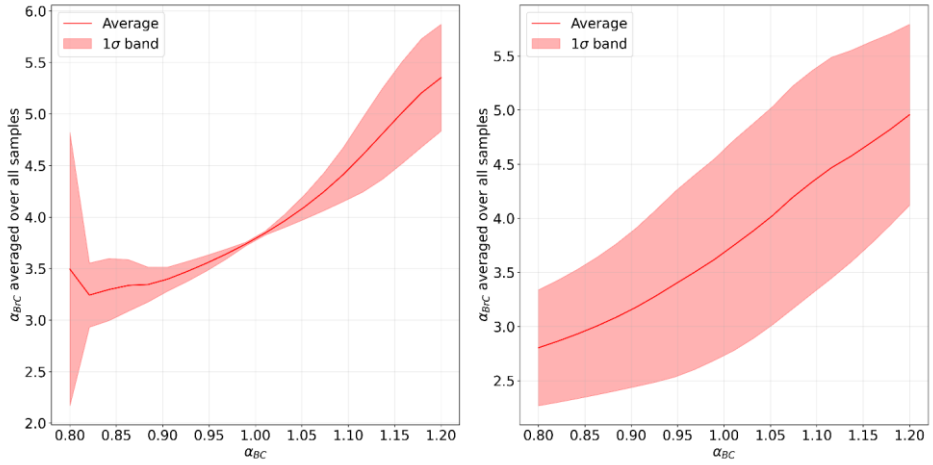

Figure S1: The α_{BC} swipe plots for the rural site (left) and the urban site (right). As can be seen by the width of the standard deviation band, this type of analysis corroborates the choice of $\alpha_{BC} = 1$ for the rural site, while proving inconclusive in the urban site where evidently the chemical composition of BrC is much more complex than in the rural site.

3 Toolkit output

The core of the analysis algorithm is represented by the optical apportionment procedure in steps II and III. Accordingly, the toolkit always provides one output .csv file for each of these runtime phases. For step II, the file `fitres.csv` is produced, which contains the fit parameters with their uncertainties for each sample; for step III, the file `appres.csv` is written, containing the apportioned optical absorption coefficient for each sample at all the wavelengths. Additionally, if step IV is enabled, a `mappres.csv` file is written with all the apportioned mass concentrations for each sample.

The toolkit always produces a `log.txt` file and a `data.pkl` file. In the log file, miscellaneous information is written, such as the input file, the working directory, the location of the written files and plots, as well as the results of the pre-processing step and the mass apportionment parameters k_1 and k_2. The data file is for internal use of the software and should be of no interest to the high-level user.

Finally, if the plots option is enabled in the configuration file, a number of subfolders containing plots for the various steps of the analysis will be created.

References

Alfaro, S. C., Lafon, S., Rajot, J. L., Formenti, P., Gaudichet, A., Maillé, M.: Iron oxides and light absorption by pure desert dust: An experimental study, J. Geophys. Res., 109, D08208, https://doi.org/10.1029/2003JD004374, 2004.

Andreae, M. O. and Gelencsér, A.: Black carbon or brown carbon? The nature of light-absorbing carbonaceous aerosol, Atmos. Chem. Phys., 6, 3131–3148, https://doi.org/10.5194/acp-6-3131-2006, 2006.

Bernardoni, V., Pileci, R. E., Caponi, L., Massabò D.: The Multi-Wavelength Absorption Analyzer (MWAA) Model as a Tool for Source and Component Apportionment Based on Aerosol Absorption Properties: Application to Samples Collected in Different Environments, Atmosphere, 8(11), :218, https://doi.org/10.3390/atmos8110218, 2017.

Bond, T. C. and Bergstrom, R. W.: Light absorption by carbonaceous particles: an investigative review, Aerosol Sci. Tech., 40, 27–67, 2006.

Bond, T. C., Doherty, S. J., Fahey, D. W., Forster, P. M., Berntsen, T., Deangelo, B. J., Flanner, M. G., Ghan, S., Kärcher, B., Koch, D., Kinne, S., Kondo, Y., Quinn, P. K., Sarofim, M. C., Schultz, M. G., Schulz, M., Venkataraman, C., Zhang, H., Zhang, S., Bellouin, N., Guttikunda, S. K., Hopke, P. K., Jacobson, M. Z., Kaiser, J. W., Klimont, Z., Lohmann, U., Schwarz, J. P., Shindell, D., Storelvmo, T., Warren, S. G., Zender, C. S.: Bounding the role of black carbon in the climate system: A scientific assessment, Journal of Geophysical Research: Atmospheres, vol. 118, no. 11, pp. 5380-5552, https://doi.org/10.1002/jgrd.50171, 2013.

Caponi, L., Formenti, P., Massabó, D., Di Biagio, C., Cazaunau, M., Pangui, E., Chevaillier, S., Landrot, G., Andreae, M. O., Kandler, K., Piketh, S., Saeed, T., Seibert, D., Williams, E., Balkanski, Y., Prati, P., and Doussin, J.-F.: Spectral- and size-resolved mass absorption efficiency of mineral dust aerosols in the shortwave spectrum: a simulation chamber study, Atmos. Chem. Phys., 17, 7175–7191, https://doi.org/10.5194/acp-17-7175-2017, 2017.

Di Biagio, C., Formenti, P., Balkanski, Y., Caponi, L., Cazaunau, M., Pangui, E., Journet, E., Nowak, S., Andreae, M. O., Kandler, K., Saeed, T., Piketh, S., Seibert, D., Williams, E., and Doussin, J.-F.: Complex refractive indices and single-scattering albedo of global dust aerosols in the shortwave spectrum and relationship to size and iron content, Atmos. Chem. Phys., 19, 15503–15531, https://doi.org/10.5194/acp-19-15503-2019, 2019.

Favez, O., El Haddad, I., Piot, C., Boreave, A., Abidi, E., Marchand, N., Jaffrezo, J.L., Besombes, J.L., Personnaz, M.B., Sciare, J., Wortham, H., Geroge, C., D'Anna, B., 2010. Inter-comparison of source apportionment models for the estimation of wood burning aerosols during wintertime in an Alpine city (Grenoble, France). Atmos. Chem. Phys. 10, 5295e5314. https://doi.org/10.1016/j.atmosenv.2009.04.035.

Forello, AC., Bernardoni, V., Calzolai, G., Lucarelli, F., Massabo, D., Nava, S., Pileci, RE., Prati, P., Valentini, S., Valli, G., Vecchi, R: Exploiting multi-wavelength aerosol absorption coefficients in a multi-time resolution source

apportionment study to retrieve source-dependent absorption parameters, Atmos. Chem. Phys. 19, 11235-11252, 10.5194/acp-19-11235-2019, 2019.

Forrister, H., Liu, J., Scheuer, E., Dibb, J., Ziemba, L., Thornhill, K. L., Anderson, B., Diskin, G., Perring, A. E., Schwarz, J. P., Campuzano-Jost, P., Day, D. A., Palm, B. B., Jimenez, J. L., Nenes, A., and Weber, R. J.: Evolution of brown carbon in wildfire plumes, Geophys. Res. Lett., 42, 4623–4630, https://doi.org/10.1002/2015GL063897, 2015.

Harris, C.R., Millman, K.J., van der Walt, S.J., Gommers, R., Virtanen, P., Cournapeau, D., Wieser, E., Taylor, J., Berg, S., Smith, N. J., Kern, R., Picus, M., Hoyer, S., van Kerkwijk, M. H., Brett, M., Haldane, A., del Río, J. F., Wiebe, M., Peterson, P., Marchant, P. G., Sheppard, K., Reddy, T., Weckesser, W., Abbasi, H., Gohlke, C., Oliphant, T. E.: Array programming with NumPy. Nature 585, 357–362, https://doi.org/10.1038/s41586-020-2649-2, 2020.

Harrison, R. M., Beddows, D. C. S., Jones A. M., Calvo A., Alves C., and Pio C.: An evaluation of some issues regarding the use of aethalometers to measure woodsmoke concentrations, Atmos. Environ., 80, 540–548, 2013.

Helin, A., Niemi, J.V., Virkkula, A., Pirjola, L., Teinilä, K., Backman, J., Aurela, M., Saarikoski, S., Rönkkö, T., Asmi, E., Timonen, H: Characteristics and source apportionment of black carbon in the Helsinki metropolitan area, Finland. Atmos. Environ. 190, 87–98. https://doi.org/10.1016/j.atmosenv.2018.07.022, 2018.

Hoffer, A., Gelencser, A., Guyon, P., Kiss, G., Schmid, O., Frank, G. P., Artaxo, P., and Andreae, M. O.: Optical properties of humic-like substances (HULIS) in biomass-burning aerosols, Atmos. Chem. Phys. 6, 3563–3570, doi:10.5194/acp-6-3563-2006, 2006.

Hunter, J. D.: "Matplotlib: A 2D Graphics Environment", Computing in Science & Engineering, vol. 9, no. 3, pp. 90-95, DOI: 10.1109/MCSE.2007.55, 2007.

Herich, H., Hueglin, C., Buchmann, B., A 2.5 year's source apportionment study of black carbon from wood burning and fossil fuel combustion at urban and rural sites in Switzerland. Atm. Meas. Tech. 4, 1409-1420, 10.5194/amt-4-1409-2011, 2011.

Ivančič, M., Gregorič, A., Lavrič, G., Alföldy, B., Ježek, I., Hasheminassab, S., Pakbin, P., Ahangar, F., Sowlat, M., Boddeker, S., Rigler, M.: Two-Year-Long High-Time-Resolution Apportionment of Primary and Secondary Carbonaceous Aerosols in the Los Angeles Basin Using an Advanced Total Carbon–Black Carbon (TC-BC(λ)) Method, Sci. Total Environ. 848, 157606, http://dx.doi.org/10.1016/j.scitotenv.2022.157606, 2022.

Lack, D. A. and Langridge, J. M.: On the attribution of black and brown carbon light absorption using the Ångström exponent, Atmos. Chem. Phys., 13, 10535–10543, https://doi.org/10.5194/acp-13-10535-2013, 2013.

Laj, P., Bigi, A., Rose, C., Andrews, E., Lund Myhre, C., Collaud Coen, M., Lin, Y., Wiedensohler, A., Schulz, M., Ogren, J. A., Fiebig, M., Gliß, J., Mortier, A., Pandolfi, M., Petäja, T., Kim, S.-W., Aas, W., Putaud, J.-P., Mayol-

Bracero, O., Keywood, M., Labrador, L., Aalto, P., Ahlberg, E., Alados Arboledas, L., Alastuey, A., Andrade, M., Artíñano, B., Ausmeel, S., Arsov, T., Asmi, E., Backman, J., Baltensperger, U., Bastian, S., Bath, O., Beukes, J. P., Brem, B. T., Bukowiecki, N., Conil, S., Couret, C., Day, D., Dayantolis, W., Degorska, A., Eleftheriadis, K., Fetfatzis, P., Favez, O., Flentje, H., Gini, M. I., Gregoric, A., Gysel- ˇ Beer, M., Hallar, A. G., Hand, J., Hoffer, A., Hueglin, C., Hooda, R. K., Hyvärinen, A., Kalapov, I., Kalivitis, N., Kasper-Giebl, A., Kim, J. E., Kouvarakis, G., Kranjc, I., Krejci, R., Kulmala, M., Labuschagne, C., Lee, H.-J., Lihavainen, H., Lin, N.-H., Löschau, G., Luoma, K., Marinoni, A., Martins Dos Santos, S., Meinhardt, F., Merkel, M., Metzger, J.-M., Mihalopoulos, N., Nguyen, N. A., Ondracek, J., Pérez, N., Perrone, M. R., Petit, J.-E., Picard, D., Pichon, J.-M., Pont, V., Prats, N., Prenni, A., Reisen, F., Romano, S., Sellegri, K., Sharma, S., Schauer, G., Sheridan, P., Sherman, J. P., Schütze, M., Schwerin, A., Sohmer, R., Sorribas, M., Steinbacher, M., Sun, J., Titos, G., Toczko, B., Tuch, T., Tulet, P., Tunved, P., Vakkari, V., Velarde, F., Velasquez, P., Villani, P., Vratolis, S., Wang, S.-H., Weinhold, K., Weller, R., Yela, M., Yus-Diez, J., Zdimal, V., Zieger, P., and Zikova, N.: A global analysis of climate-relevant aerosol properties retrieved from the network of Global Atmosphere Watch (GAW) near-surface observatories, Atmos. Meas. Tech., 13, 4353–4392, https://doi.org/10.5194/amt-13-4353-2020, 2020.

Liu, S., Aiken, A. C., Gorkowski, K., Dubey, M. K., Cappa, C. D., Williams, L. R., Herndon, S. C., Massoli, P., Fortner, E. C., Chhabra, P. S., Brooks, W. A., Onasch, T. B., Jayne, J. T., Worsnop, D. R., China, S., Sharma, N., Mazzoleni, C., Xu, L., Ng, N. L., Liu, D., Allan, J. D., Lee, J. D., Fleming, Z. L., Mohr, C., Zotter, P., Szidat, S., Prévôt, A. S. H.: Enhanced light absorption by mixed source black and brown carbon particles in UK winter, Nature Communications, volume 6, Article number: 8435, https://doi.org/10.1038/ncomms9435, 2015.

Liu, J., Bergin, M., Guo, H., King, L., Kotra, N., Edgerton, E., Weber, R. J.: Size-resolved measurements of brown carbon in water and methanol extracts and estimates of their contribution to ambient fine-particle light absorption, Atmos. Chem. Phys., 13, 12389–12404, https://doi.org/10.5194/acp-13-12389-2013, 2013.

Martinsson, J., Abdul Azeem, H., Sporre, M.K., Bergström, R., Ahlberg, E., Öström, E., Kristensson, A., Swietlicki, E., Eriksson Stenström, K.: Carbonaceous aerosol source apportionment using the aethalometer model – evaluation by radiocarbon and levoglucosan analysis at a rural background site in southern Sweden. Atmos. Chem. Phys. 17, 4265–4281. https://doi.org/10.5194/acp-17-4265-2017, 2017.

Massabò, D., Bernardoni, V., Bove, M. C., Brunengo, A., Cuccia, E., Piazzalunga, A., Prati, P., Valli, G., Vecchi, R.: A multi-wavelength optical set-up for the characterization of carbonaceous particulate matter, Journal of Aerosol Science, 60, 34-46, https://doi.org/10.1016/j.jaerosci.2013.02.006, 2013.

Massabò, D., Caponi, L., Bernardoni, V., Bove, M. C., Brotto, P., Calzolai, G., Cassola, F., Chiari, M., Fedi, M., Fermo, P., Giannoni, M., Lucarelli, F., Nava, S., Piazzalunga, A., Valli, G., Vecchi, R., Prati, P.: Multi-wavelength optical determination of black and brown carbon in atmospheric aerosols, Atmospheric Environment, 108, 1-12, https://doi.org/10.1016/j.atmosenv.2015.02.058, 2015.

Codice campo modificato

Massabò, D., Altomari, A., Vernocchi, V., and Prati, P.: Two-wavelength thermal–optical determination of light-absorbing carbon in atmospheric aerosols, Atmos. Meas. Tech., 12, 3173–3182, https://doi.org/10.5194/amt-12-3173-2019, 2019.

Minderytė, A., Pauraite, J., Dudoitis, V., Plauškaitė, K., Kilikevičius, A., Matijošius, J., Rimkus, A., Kilikevičienė, K., Vainorius, D., Byčenkienė, S.: Carbonaceous aerosol source apportionment and assessment of transport-related pollution, Atmos. Env., 279, 119043, ISSN 1352-2310, https://doi.org/10.1016/j.atmosenv.2022.119043, 2022.

Moosmüller, H., Chakrabarty, R. K., Ehlers, K. M., and Arnott, W. P.: Absorption Ångström coefficient, brown carbon, and aerosols: basic concepts, bulk matter, and spherical particles, Atmos. Chem. Phys., 11, 1217–1225, https://doi.org/10.5194/acp-11-1217-2011, 2011.

Piazzalunga, A., Fermo, P., Bernardoni, V., Vecchi, R., Valli, G., De Gregorio M. A.: A simplified method for levoglucosan quantification in wintertime atmospheric particulate matter by high performance anion-exchange chromatography coupled with pulsed amperometric detection, Int. J. Environ. An. Ch., 90, 934–947, https://doi.org/10.1080/03067310903023619, 2010.

Poeschl, U., 2003, Aerosol particle analysis: challenges and progress, Anal. Bioanal. Chem. 375, 3032, 10.1007/s00216-002-1611-5, 2003.

Reback J., jbrockmendel, McKinney, W., Van den Bossche, J., Roeschke, M., Augspurger, T., Hawkins, S., Cloud, P., gfyoung, Sinhrks, Hoefler, P., Klein, A., Petersen, T., Tratner, J., She, C., Ayd, W., Naveh, S., Darbyshire, J. H. M., Shadrach, R., Li, T.: pandas-dev/pandas: Pandas 1.4.3 (v1.4.3). Zenodo [code]. https://doi.org/10.5281/zenodo.6702671, 2022.

Sandradewi J., Prévôt A. S., Szidat S., Perron N., Alfarra M. R., Lanz V. A., Weingartner E., Baltensperger U.: Using aerosol light absorption measurements for the quantitative determination of wood burning and traffic emission contributions to particulate matter. Environ Sci Technol. May 1;42(9):3316-23, doi: 10.1021/es702253m. PMID: 18522112, 2008.

Schepanski, K. Transport of Mineral Dust and Its Impact on Climate. Geosciences, 8, 151. https://doi.org/10.3390/geosciences8050151, 2018.

Simoneit, B. R. T., Schauer, J. J., Nolte, C. G., Oros, D. R., Elias, V. O., Fraser, M. P., Rogge, W. F., & Cass, G. R.: Levoglucosan, a tracer for cellulose in biomass burning and atmospheric particles. Atmospheric Environment, 33(2), 173-182, https://doi.org/10.1016/S1352-2310(98)00145-9, 1999.

Seinfeld, J. and Pandis, S.: Atmospheric Chemistry and Physics: from air pollution to climate change, Wiley & Sons, ISBN 978-1-118-94740-1, 2016.

Tang, M., Alexander, J. M., Kwon, D., Estillore, A. D., Laskina, O., Young, M. A., Kleiber, P. D., and Grassian, V. H.: Optical and Physicochemical Properties of Brown Carbon Aerosol: Light Scattering, FTIR Extinction Spectroscopy, and Hygroscopic Growth, J. Phys. Chem. A, 120 (24), 4155-4166, DOI: 10.1021/acs.jpca.6b03425, 2016.

Utry, N., Ajtai, T., Filep, A, Pinter, M., Torok, Zs, Bozoki., Z., Szabo, G.: Correlations between absorption Angström exponent (AAE) of wintertime ambient urban aerosol and its physical and chemical properties, Atmos. Environ. 91, 52-59, https://doi.org/10.1016/j.atmosenv.2014.03.047, 2013.

Vernocchi, V., Brunoldi, M., Danelli, S. G., Parodi, F., Prati, P., Massabò, D.: Characterization of soot produced by the mini-inverted soot generator with an atmospheric simulation chamber, Atmos. Meas. Tech., 15, 2159–2175, https://doi.org/10.5194/amt-15-2159-2022, 2022.

Virtanen, P., Gommers, R., Oliphant, T. E., Haberland, M., Reddy, T., Cournapeau, D., Burovski, E., Peterson, P., Weckesser, W., Bright, J., van der Walt, S. J., Brett, M., Wilson, J., Millman, K. J., Mayorov, N., Nelson, A. R. J., Jones, E., Kern, R., Larson, E., Carey, C. J., Polat, İ., Feng, Y., Moore, E. W., VanderPlas, J., Laxalde, D., Perktold, J., Cimrman, R., Henriksen, I., Quintero, E. A., Harris, C. R., Archibald, A. M., Ribeiro, A. H., Pedregosa, F., van Mulbregt, P., and SciPy 1.0 Contributors.: SciPy 1.0: Fundamental Algorithms for Scientific Computing in Python. Nature Methods, 17(3), 261-272, https://doi.org/10.1038/s41592-019-0686-2, 2020

Zotter, P., Herich, H., Gysel, M., El-Haddad, I., Zhang, YL., Mocnik, G., Huglin, C., Baltensperger, U., Szidat, S., Prevot, AH: Evaluation of the absorption angstrom exponents for traffic and wood burning in the Aethalometer-based source apportionment using radiocarbon measurements of ambient aerosol, Atmos. Chem. Phys., 17, 4229-4249, DOI: 10.5194/acp-17-4229-2017, 2017.